Large scale 1-g shake table model test on the response of a stiff pile group to liquefaction induced lateral spreading

Réponse d'un groupe de 3 × 3 pieux rigides sous l'action d'un écoulement latéral induit par liquéfaction étudié à grande échelle sur table vibrante

Haeri S.M., Kavand A., Asefzadeh A.
Department of civil engineering, Sharif University of Technology, Tehran, Iran
Rahmani I.
Marine transportation and technology division, Transportation research institute, Tehran, Iran

ABSTRACT: Evaluation of pile response to liquefaction induced lateral spreading is an important step towards resistant design of pile foundations against this destructive phenomenon. This paper investigates the response of a stiff 3×3 pile group under liquefaction induced lateral spreading using large scale 1-g shake table test. The model ground consisted of a 3-layer soil profile including a base non-liquefiable layer, a middle liquefiable layer and an upper non-liquefiable layer. Different parameters of the response of laterally spreading soil as well as those of the pile group including accelerations, pore water pressures, displacements and bending moments were recorded during the shaking that are presented and discussed in the paper. In addition, distribution of lateral pressures due to lateral spreading on individual piles of the group is investigated in detail. The results show that lateral forces exerted by the laterally spreading soil vary in the individual pile of the group both in transverse and longitudinal directions depending on the pile position within the group. It was also found that the magnitude of lateral pressures due to lateral spreading on the stiff 3×3 pile group of this study are close to the values recommended by the design code.

RÉSUMÉ : L'évaluation de la réponse d'un pieu à l'écoulement latéral induit par liquéfaction est une étape importante vers la conception de fondations sur pieux contre ce phénomène destructeur. Cet article présent l'étude de la réponse d'un groupe de 3 × 3 pieux rigides en vraie grandeur à 1 g sur table vibrante. Le modèle de sol est composé de 3 couches comprenant une couche centrale liquéfiable et des épontes non liquéfiables. Différents paramètres de la réponse du sol ainsi que ceux du groupe de pieux, y compris les accélérations, les pressions interstitielles, les déplacements et les moments de flexion ont été enregistrés pendant l'essai et sont présentés et discutés dans cet article. De plus, la distribution des pressions latérales de sol dues à l'écoulement sur tous les pieux du groupe est étudiée en détail. Les résultats montrent que les forces latérales exercées par le sol écoulé varient dans le pieu individuel du groupe à la fois dans les directions transversale et longitudinale, selon la position du pieu à l'intérieur du groupe. Il a également été constaté que la valeur des pressions latérales dues au sol écoulé sur le groupe de pieux sont proches des valeurs recommandées par le code de conception.

KEYWORDS: Pile group, liquefaction, lateral spreading, 1-g shake table test.

1 INTRODUCTION

Liquefaction-induced lateral spreading is commonly observed in gently sloping grounds or lands ending in free faces as a result of liquefaction in underlying saturated loose cohesionless deposits. In these deposits, earthquake-induced excess pore water pressures can cause a significant decrease in soil shear strength resulting in ground movement towards downslope or free face due to existing static shear forces (Kramer and Elgamal 2001). Lateral spreading can impose significant lateral pressures on pile foundations. During past earthquakes, several examples regarding severe damages to piles and structures supported on them due to lateral spreading have been documented, among which the cases in the 1964 Niigata (Hamada et al. 1986), the 1995 Kobe (Tokimatsu and Asaka 1998), and the 2010 Haiti earthquakes (Eberhard Marc et al. 2010) are the most important ones in this respect.

Although some experimental studies including shaking table, centrifuge and field tests (e.g. Haeri et al. 2012, Motamed and Towhata 2010, Abdoun et al. 2003, Ashford et al. 2006) have been conducted to evaluate the response of pile groups to lateral spreading, but different aspects of the soil-pile interaction in laterally spreading ground are not yet fully understood. For example, there are not still enough effective researches concerning variation of the value and pattern of the lateral pressures from the liquefied layer against different individual piles of a group. Motamed and Towhata [10] recently showed that the lateral spreading force in an individual pile within a group varies depending on the pile position in the group. They conducted a series of 1-g shaking table tests on pile groups behind quay walls in a two-layer soil profile, including a non-liquefiable layer overlain by a top liquefiable layer, and showed that in a pile group rear-row piles which are closer to the quay wall sustain larger lateral pressures, while front-row piles sustain smaller values.

In this paper response of a stiff 3×3 pile group under liquefaction induced lateral spreading in a 3-layer soil profile including a base non-liquefiable layer, a middle liquefiable layer and an upper non-liquefiable layer is studied. For this purpose 1-g shake table physical modeling is utilized. Different parameters of the response of laterally spreading soil as well as those of the pile group such as accelerations, pore water pressures, bending moments and displacements were recorded during the test that are briefly discussed in the paper. The main focus of this paper is on distribution of lateral soil forces in individual piles of the group.

2 PHYSICAL MODEL

The experiment of this study was conducted using shaking table device of the earthquake research center at Sharif University of Technology (SUT).

In order to hold the physical model, a rigid box was used which had a length of 3.5 m, width of 1 m and height of 1.5 m. Figure 1 shows the schematic cross section and plan view of the physical model along with the layout of transducers. As seen, the soil profile consists of three distinct layers including a non-liquefiable crust with a thickness of 25 cm and relative density of about 60%, that is made of sand and clay (10% by weight of sand); a 1m thick middle liquefiable layer consisting of loose sand with relative density of about 15% and a lower non-liquefiable dense sand layer having 25 cm thickness and relative density of about 80%. All the soil layers have a slope of 7%. The sand used in physical model is standard Firoozkuh silica sand (No. 161) which has a uniform grain size distribution and is widely used in Iran for geotechnical physical modeling.

Model piles of this study were initially designed as steel piles in prototype scale according to recommendations by JRA 2002 since representing a stiff pile comparing to concrete ones. Subsequently, mechanical and geometrical properties of the piles were calculated in model scale using similitude laws proposed by Iai et al. (2005). In this regard, the geometrical scale was selected as λ=8 (prototype/model). All model piles were made of aluminum pipes. Material properties of the model piles are summarized in Table 1.

As sketched in Figure 1, various types of transducers were employed in different parts of the model including accelerometers and pore pressure transducers in the free field (far from the piles) to measure soil accelerations and excess pore water pressures; pore pressure transducers close to the piles to monitor build-up and dissipation of the excess pore pressures in the near field (close to the piles); displacement transducers (LVDTs) attached to the pile cap and also in free field to record pile and soil lateral displacements and finally strain gauges pasted along the piles to record bending moments. Base excitation was applied parallel to the model slope. The excitation was a sinusoidal acceleration record having amplitude of 0.3g and frequency of 3 Hz whose duration was 12 sec consisting of two rising and falling parts, each of duration of about 1.0 sec at the beginning and end of shaking.

Table 1. Mechanical and geometrical properties of pile foundations.

Material	Height (m)	Outer/inner diameter (cm)	I (cm4)	EI (kN.m2)
Aluminum	1.25	5.2/4.7	5.904	4.054

3 SUMMARY OF EXPERIMENTAL RESULTS

In this section a summary of the main measured data during the shaking table test is briefly presented and discussed.

3.1. Soil acceleration in free field

Sample soil acceleration time histories in the free field part of the model (soil far from the piles) are shown in Figure 2. As can be observed in this figure, the amplitude of acceleration records in liquefiable layer decreased dramatically at the beginning stages of shaking as the soil underwent liquefaction.

3.2. Excess pore water pressure records

Representative excess pore pressure time histories recorded in free field area are shown in Figure 3. The trends show that the soil liquefied after about 3 cycles of shaking since the middle layer composed of very loose sand. Drainage of excess pore pressures or consolidation of the liquefied sand initiated from the lower depths (PWP1) and followed by pore pressure reduction in upper elevations (PWP2).

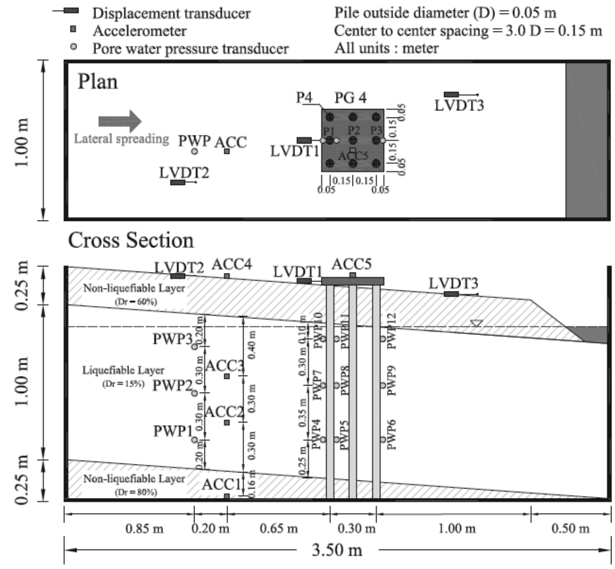

Figure 1. Plan view and cross section of the physical model.

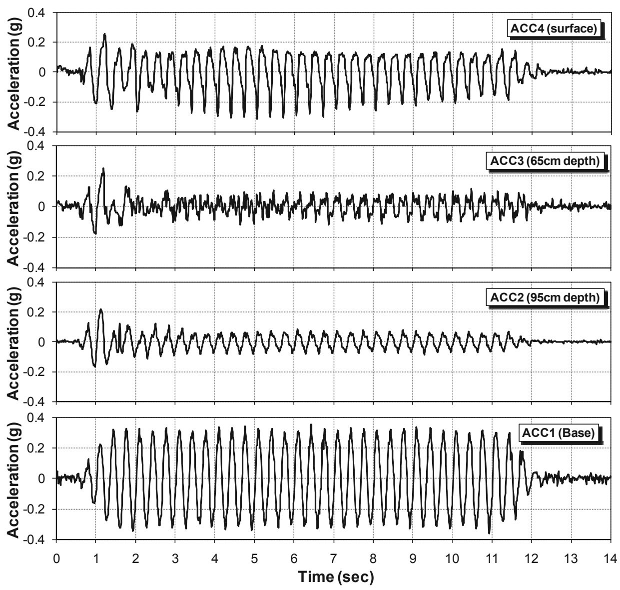

Figure 2. Sample acceleration time histories of soil in the free field.

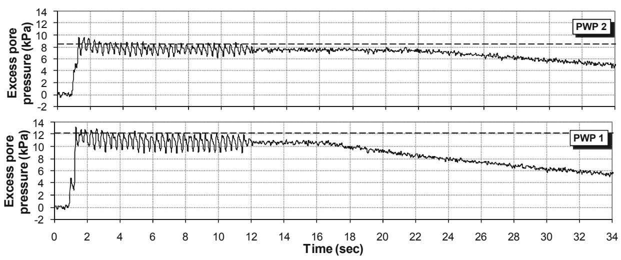

Figure 3. Sample excess pore water pressure records in free field.

3.3. Soil and pile group lateral displacement records

Figure 4, summarizes displacement records of the pile cap and soil at the free field. As seen, the soil started to move downward right after being liquefied. Unlike the free field soil displacement which kept increasing until the end of shaking, pile cap displacement reached its maximum displacement a few seconds after the shaking and then bounced back gradually having a residual displacement of about 9 mm. The maximum ground surface displacement was about 5.0 cm while the maximum displacement of the cap was about 5.4 cm.

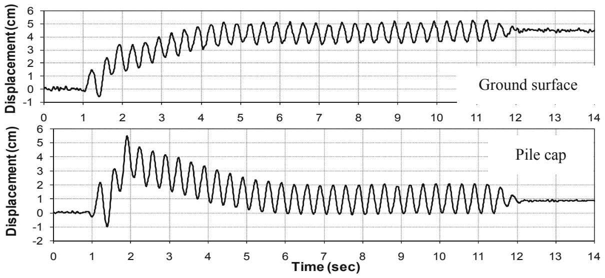

Figure 4. Time histories of ground surface and lateral pile cap displacements.

3.4. Pile bending moments

Figure 5 shows time histories of bending moments in instrumented individual piles of the group at some representative depths, i.e. at base of the liquefiable layer and near the connection of piles to the cap. As seen, after lateral spreading that occurred about t=1.5 sec, bending moments increases significantly. However, during liquefaction, the soil loses most of its shear resistance; hence it fails and gradually moves around the piles. This movement reduces the lateral pressure on the piles; therefore the piles bounce back towards upslope due to their rigidity as the shaking continued. Due to this elastic rebound, bending moments in piles descend as well. It should be noted that time histories of bending moments in all piles consist of a cyclic component due to dynamic soil pressures as well as a monotonic component from the kinematic lateral soil pressures during lateral spreading. An interesting observation is that maximum positive bending moments differ in individual piles of the group depending on their position within the group.

4 LATERAL PRESSURE OF LIQUEFIED SOIL ON THE PILES

The lateral pressures exerted on the individual piles of the groups were back-calculated from the monotonic component of bending moment data using the method introduced by Brandenberg et al. (2010). Figure 6 shows profiles of the monotonic component of back-calculated lateral pressures of liquefied soil along with the lateral forces proposed by JRA (2002) code for design of pile groups against lateral spreading. This code recommends using 30% of the total overburden pressure to be applied to the outermost width of the pile group as lateral forces due to lateral spreading. In cases with a top non-liquefiable layer, it suggests that the passive pressure from non-liquefiable layer should be considered as well. For design applications, implementing JRA (2002), it is assumed that the total lateral force exerted on the pile group is equally distributed among the individual piles of the group.

According to Figure 6, at the early stages of shaking when the soil was not yet liquefied, induced pressures are negligible. But upon liquefaction and lateral spreading, magnitude of lateral pressures increased significantly. In all diagrams, an increase in applied lateral pressures is observed at upper elevations where the non-liquefiable crust exists. In fact, the non-liquefiable crust moved with the underlying liquefied layer towards the downslope during lateral spreading, exerting extra pressures on the piles. As seen in Figure 6, the magnitude of lateral pressures on pile 3 (the downslpe pile) in upper elevations are greater than those of the other piles which can be attributed to the separation of the soil from the downslope side of pile 3 during lateral spreading resulting in lack of lateral support. The agreement between the magnitudes and patterns of back-calculated lateral pressures with the values recommended by JRA 2002 is reasonable except in pile 3 which shows significant difference with JRA 2002 values in terms of pressure magnitude and pattern.

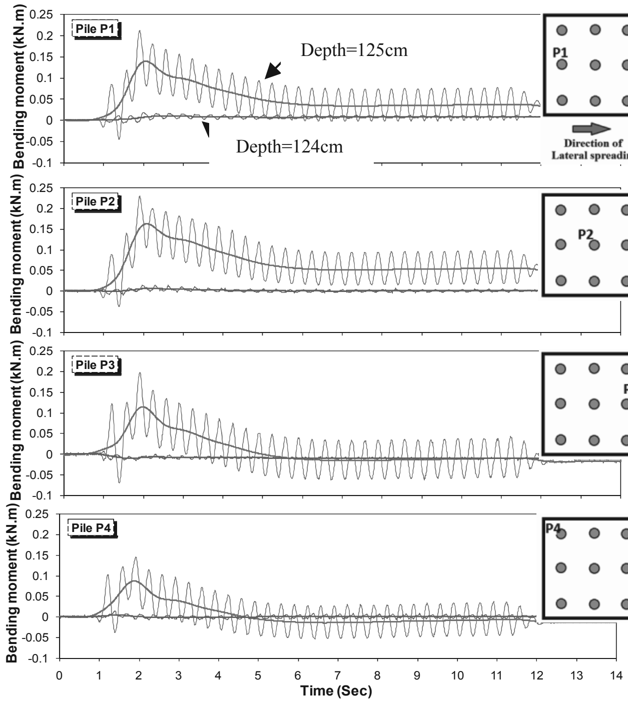

Figure 5. Time histories of bending moments in representative individual piles of the group.

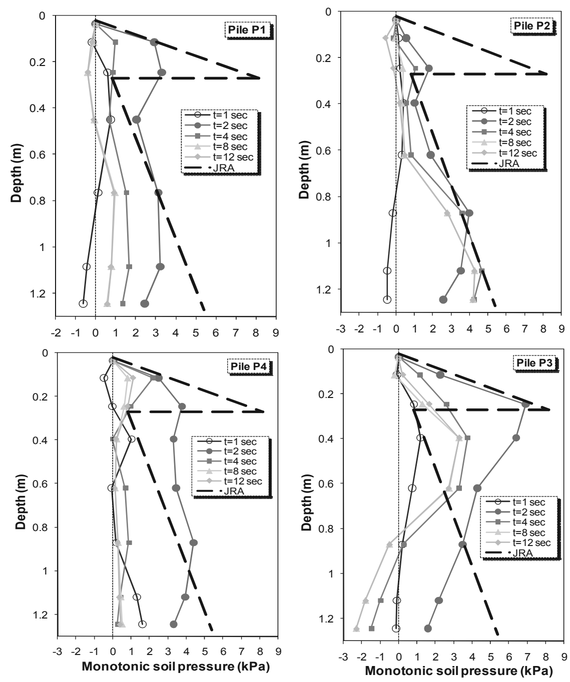

Figure 6. Profiles of lateral soil pressures on individual piles of the group during lateral spreading.

3.5. Total lateral forces exerted on individual piles

Monotonic components of maximum total lateral forces exerted on the piles were calculated by integrating the lateral soil pressures along the piles. These total lateral forces were separately evaluated for the liquefied layer and the non-liquefiable crust. The calculated forces are displayed in Figure 7. By comparing total lateral forces in different piles following findings can be itemized:

- The amount of total lateral force in pile P2 (located in middle row) is less than the piles located in upslope and downslope rows, i.e. piles P1 and P3.
- Total lateral force on pile P1 is about 1.24 times that exerted on pile P2. This occurs due to the shadow effect. Since the upslope pile is directly pushed by the laterally spreading soil and acts as a barrier for pile downslope pile, P2.
- Total lateral force exerted on pile P3 is the largest among all the other piles. Total lateral force on pile P3 is about 1.43 and 1.76 times those of piles P1 and P2, respectively. This can be described by the separation of soil from the downslope side of pile P3 during lateral spreading resulting in lack of lateral support.
- Comparing total lateral forces in pile P1 (the middle pile in upslope row) and P4 (the side pile in upslope row) shows that the side pile receives larger force than the middle pile by a factor of about 1.27. This phenomenon is called neighboring effect.

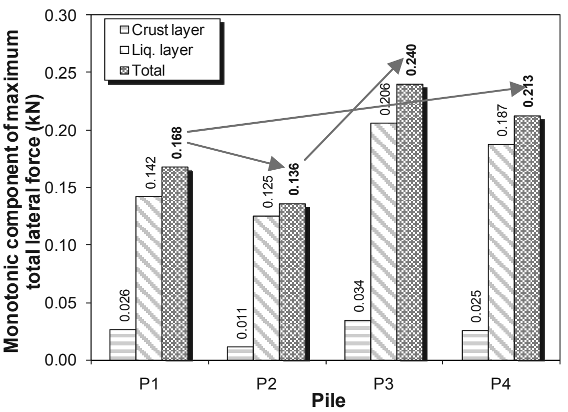

Figure 7. Comparison of maximum total lateral forces on different piles of the group.

3.6. Total lateral force exerted on the pile group

Total lateral forces exerted on the group can be estimated by adding all lateral forces exerting on individual piles of the group. It should be noted that in this experiment, only one side pile in upslope row of the group was instrumented but it was assumed that the ratio of lateral forces on the side piles of other rows to those of their corresponding middle piles is the same as the ratio between piles P4 and P1. Total forces exerted on pile group of this experiment are compared with those recommended by JRA 2002 in Figure 8. According to this figure, total lateral force exerted on the pile group is about 1.04 times the values calculated using recommendations of JRA 2002. This difference in total lateral forces is found to be negligible. But if only the lateral forces from the liquefiable layer be considred the differences will be more. However, the trend observed for the non-liquefiable crust layer is completely different as the lateral forces suggested by JRA [2002] is about 2.2 times the experimental values. The reason is that passive pressure recommended by JRA 2002 does not seem to be mobilized in this experiment.

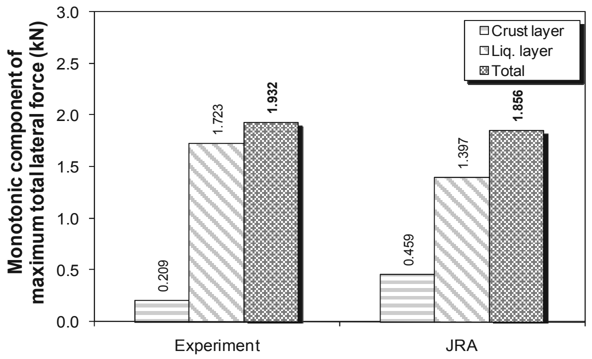

Figure 8. Comparison between monotonic components of maximum total lateral forces in pile group of this experiment and JRA 2002 recommended values.

4. CONCLUSIONS

Findings from a large scale shake table test on a stiff 3×3 pile group are presented and disscussed. The results show that total lateral forces due to lateral spreading on the pile group can be well predicted by JRA 2002 design code. However, based on the experimental results, lateral forces exerted on individual piles of the group varries depending on the pile positions within the group which is not considered by JRA code. The shadow and neighboring effects are found to be responsible for such an observation. It is recommended that this variation be considered in design applications.

5. REFERENCES

Kramer S.L. and Elgamal, A. 2001. Modeling soil liquefaction hazards for performance-based earthquake engineering. PEER report 2001/13, Pacific Earthquake Engineering Research Center, College of Engineering, Univ. of California, Berkeley.

Hamada H., Yasuda S., Isoyama R. and Emoto K. 1986. Study on Liquefaction Induced Permanent Ground Displacements. Research report, Association for the Development of Earthquake Prediction, Japan.

Tokimatsu K. and Asaka Y. 1998. Effects of Liquefaction-Induced Ground Displacements on Pile Performance in the 1995 Hyogoken-Nambu Earthquake. Special Issue of Soils and Foundations, pages 163–177.

Eberhard Marc O., Baldridge S., Marshall J., Mooney W. and Rix J. 2010. USGS/EERI Advance Reconnaissance Team: TEAM REPORT V 1.1, The MW 7.0 Haiti Earthquake of January 12, 2010.

Haeri S. M., Kavand A., Rahmani I. and Torabi H. 2012. Response of a group of piles to liquefaction-induced lateral spreading by large scale shake table testing. Soil Dynamics and Earthquake Engineering 38, 25-45.

Motamed R. and Towhata I. 2010. Shaking table model tests on pile groups behind quay walls subjected to lateral spreading. Journal of Geotechnical and Geoenvironmental Engineering 136(3), 477-489.

Abdoun T., Dobry R., O'Rourke T. and Goh SH. 2003. Pile response to lateral spreads: centrifuge modeling. Journal of Geotechnical and Geoenvironmental Engineering 129(10), 869-678.

Ashford S. A., Juirnarongrit T., Sugano T. and Hamada M. 2006. Soil–pile response to blast-induced lateral spreading. I: Field Test. Journal of Geotechnical and Geoenvironmental Engineering 132(2), 152-162.

JRA. 2002. Seismic design specifications for highway bridges. Japan Road Association, English version, Prepared by Public Works Research Institute (PWRI) and Ministry of Land, Infrastructure and Transport, Tokyo, Japan.

Iai S., Tobita T. and Nakahara T. (2005. Generalized scaling relations for dynamic centrifuge tests. Geotechnique 55(5), 355-362.

Brandenberg S. J., Wilson D. W., and Rashid M. M. 2010. Weighted residual numerical differentiation algorithm applied to experimental bending moment data. Journal of Geotechnical and Geoenvironmental Engineering 136(6), 854-863.